APPLICATION OF ULTRA-LIGHT WEIGHT FIBER REINFORCED CONCRETE FOR THE INCREASED EARTHQUAKE RESISTING WALLS

Yoshinori KITSUTAKA[1] And Tokunao OH-OKA[2]

SUMMARY

This study aims to apply concrete containing foamed waste glass aggregate (hereafter referred to as foamed aggregate concrete) to increased shear walls. Since foamed aggregate concrete exhibits a brittle failure mode, concrete containing discrete vinylon fibers was also prepared and subjected to ductility tests by center-point loading on notched beams and horizontal loading tests to confirm its effectiveness for shear walls. These tests revealed that foamed aggregate concrete sufficiently functions as supplementary shear walls, that the inclusion of vinylon fibers significantly improves the ductility and that the yield strength of such shear walls does not decrease abruptly after reaching its peak.

INTRODUCTION

Among glass bottles reclaimed for recycling, colored bottles, such as for wine, ampuled liquid medicine and cosmetics, are hardly recyclable and mostly doomed to disposal. Being made from such discarded glass bottles, foamed waste glass aggregate used in this study is not only effective in reducing the weight of concrete but also is worth utilizing from the standpoint of global environment protection.

The purpose of this study is to apply concrete containing foamed waste glass aggregate having a unit mass of 1.1 to 1.3 ton/m^3 and reasonable compressive strength to supplementary shear walls for existing buildings.

Due to the low strength of foamed waste glass aggregate, concrete containing such aggregate exhibits a more brittle failure mode than normal aggregate concrete. The authors therefore investigated the inclusion of discrete vinylon fibers as well.

This paper reports on the ductility evaluation by center-point loading on notched beams, as well as horizontal loading tests on wall specimens to confirm the effectiveness as shear walls, with their relationship investigated.

CHARACTERISTICS OF FOAMED WASTE GLASS AGGREGATE

Tables 1 and 2 give the chemical composition of foamed waste glass aggregate and aggregate test results, respectively. No.1, No.2 and No. 3 foamed waste glass aggregates were blended at a ratio of 8:1:1 to be used as fine aggregate for concrete.

[1] Department of Architecture and Building Science, Tokyo Metropolitan University, Japan Email: kitsu@arch.metro-u.ac.jp
[2] Institute of Technology, Tokyu Construction Co. Ltd., Japan Email: oooka@hd.tokyu-cnst.co.jp

Table 1: Chemical composition of foamed waste glass aggregate. (%)

ig. loss	SiO_2	Al_2O_3	Fe_2O_3	MgO	CaO	Na_2O	K_2O	SO_3
0.2	71.0	4.4	0.40	0.57	9.4	12.0	1.2	0.43

Table 2: Aggregate test results of foamed waste glass aggregate.

Type	Diameter (mm)	Gravity (Saturated and Surface-dry)	Gravity (Bone-dry)	24hours Absorption (%)	Bulk Density (ton/m^3)	Passing Standard Seive 74μm (%)
No.1	-1.2	0.81	0.75	7.85	0.46	3.7
No.2	1.2-2.5	0.70	0.65	7.18	0.38	2.6
No.3	2.5-5.0	0.66	0.61	7.64	0.34	1.5

Table 3: Mixture proportions of concretes.

Mixture Type	W/C (%)	W	C	S	G	GL	SM	VF1500	VF350	SP (C×%)
N	54	195	359	811	887	-	-	-	-	0.3
L	35	170	486	-	-	364	124	-	-	2.0
LV	35	170	486	-	-	359	122	13	-	2.0
LM	30	180	600	-	-	413	-	-	13	3.0

C: High-early-strength Portland Cement□ S: Fine Aggregate (Manufactured Sand : Pit Sand =3:7)
G: Coarse Aggregate (Crushed Sand Stone) dmax=10mm, SP: High-range water reducer (L, LV, LM), Water reducer (N□
GL: foamed waste glass aggregate, SM: Ultra-light expanded shale aggregate, VF1500□VF350: Vinylon fiber

Table 4: Physical properties of discrete vinylon fibers.

Fiber Type	Length (mm)	Diameter (μm)	Tensile Strength (MPa)	Young's Modulus (GPa)	Specific Gravity
VF1500	30	240×720	882	29	1.30
VF350	12	200			

TYPE OF SPECIMENS

Four types of concrete were used: normal concrete (N), foamed aggregate concrete (L), vinylon fiber reinforced foamed aggregate concrete (LV) and vinylon fiber reinforced foamed aggregate mortar (LM). Five column-wall specimens were prepared: a specimen with no wall (WF), with a wall of N concrete (WN), with a wall of L concrete (WL), with a wall of LV concrete (WV) and with a wall of precast panels made of LM mortar (WM).

CENTER POINT LOADING TEST ON NOTCHED BEAMS

Procedure:
Center-point loading tests on notched beams were conducted in accordance with the RILEM method [RILEM, 1985] to grasp the ductility performance of concretes used for column-beam specimens.

Tables 3 and 4 give the mixture proportions of concretes and physical properties of discrete vinylon fibers. Bending tests were conducted simultaneously with the horizontal loading test on each column-wall specimen. Six each of N and LM specimens and 3 each of L and LV specimens were tested between 22 and 42 days. The beam specimens, 100 by 100 by 500 mm in size, were seal-cured in the field in the same environment as the column-wall specimens. Notches were cut to a depth of 50 mm immediately before testing. As shown in Figure 1, beams were loaded over a span of 400 mm with an Instron-type testing machine. The loading rate was 0.02 mm/min for N and L and 0.2 mm/min for LV and LM controlled by the crosshead speed.

Strength test results of specimens for control:
Table 5 gives the strength test results of cylindrical specimens for strength control φ10 by 20 cm in size. These tests were conducted simultaneously with horizontal loading tests on column-wall specimens.

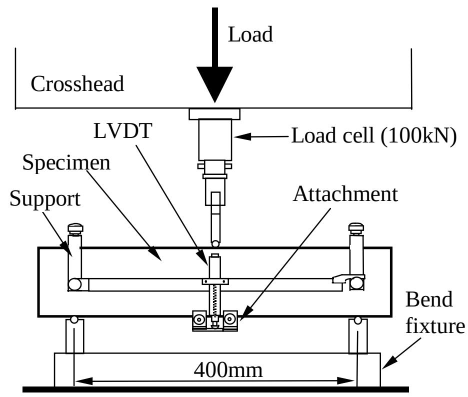

Instron universal testing instrument (Capacity100kN)

Figure 1: Three-point bending test

Table 5: Strength test results of cylindrical specimens for strength control

Specimen Type	Members	Mixture Type	Compressive Strength (MPa)	Tensile Strength (MPa)	Young's Modulus (GPa)	Bulk Density (ton/m^3)
WF	Column, Beam	N	26.7	2.41	20.4	2.24
WN	Column, Beam, Wall	N	28.6	2.21	21.9	2.25
WL	Column, Beam	N	31.7	2.75	23.3	2.17
	Wall	L	29.3	1.98	11.4	1.17
WV	Column, Beam	N	28.5	2.49	22.7	2.21
	Wall	LV	23.2	2.37	8.2	1.10
WM	Column, Beam	N	31.7	2.44	23.6	2.22
	Wall	LM	35.8	2.78	12.9	1.27
	Grout	-	47.6	-	23.4	2.15

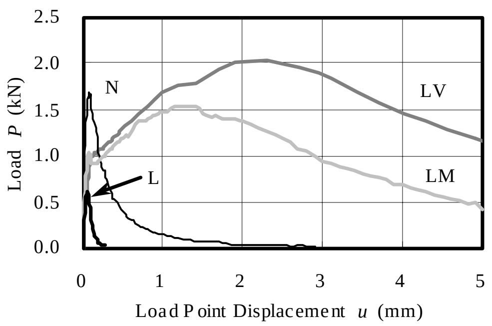

Figure 2: L-LPD curve

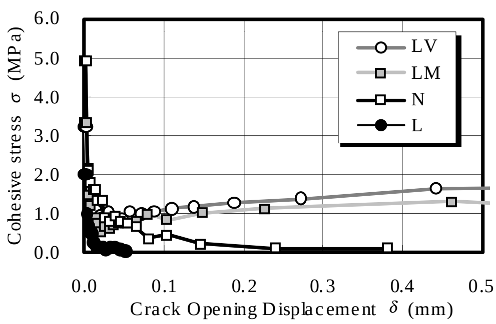

Figure 3: Tension softening diagram (TSD)

Bending test results of notched beams:

Figure 2 shows the load-load point displacement diagram (LPD) obtained from bending tests on notched beams.

Table 6: Averages of fracture parameters

Mixture Type	Young's Modulus	Fracture Energy *1	Effective Fracture Energy *2	Initial Cohesive Stress	Critical Crack Opening Displacement	Effective Tensile Strength*3	Critical Load Point Displacement	Equivalent Flexural Strength
	E (GPa)	G_F^{WOF} (N/m)	G_F^u (N/m)	σ_0 (MPa)	δ_C (mm)	f_t^{eff} (MPa)	u_0 (mm)	f_b (MPa)
N	21.11	134.7	141	4.43	0.349	2.68	2.92	4.20
L	8.37	24.3	14.9	1.39	0.050	0.96	0.29	1.55
LV	6.66	-	679	3.25	1.766	2.13	-	4.89
LM	10.92	-	558	3.34	0.892	1.84	-	3.88

*1: Calculated using RILEM method

*2: $G_F^u = \int_0^{\delta u} \sigma(\delta) d\delta$, $\delta u = 0.5mm$ *3: $f_t^{eff} = \int_0^{g_1} \sigma(\delta) d\delta \Big/ g_1$, $g_1 = 0.01\,mm$

Figure 3 shows the tension softening diagram (TSD) polylinearly approximated by inverse analysis [Kitsutaka, 1993][Kitsutaka, 1997]. The LPD indicates averages of test results of three or six specimens. The TSD was determined from the averaged LPD.

The method of calculating the fracture parameters is the same as our previous study [Kitsutaka, 1997]. Table 6 tabulates the averages of fracture parameters calculated for individual specimens. Figure 4 shows the effective fracture energy (G_F^u), effective tensile strength (f_t^{eff}) and equivalent flexural strength (f_b) of each type of concrete. Whereas the compressive strengths of N and L are similar as shown in Table 5, f_t^{eff}, f_b and G_F^u of L are lower than those of N as shown in Figure 4. These weaknesses are significantly improved by the inclusion of vinylon fibers, such as in LV.

HORIZONTAL LOADING TESTS ON COLUMN-WALL SPECIMENS

Materials:
Table 7 gives the material characteristics of reinforcing bars. Concretes were proportioned as given in Table 3, and their strengths are as given in Table 5.

Geometry of specimens:
Specimens for horizontal loading tests are given in Table 8. Figure 5 shows their geometry and typical reinforcement arrangement. Five specimens reduced to a scale of 1/3 were prepared. The overall length including the columns, distance between columns on centers, distance from the column base to the vertical center of the upper stub wall were 2,240 mm, 2,000 mm and 1,400 mm, respectively. The shear span-depth ratio was 0.625. The columns have a square cross-section 240 by 240 mm in size. The thickness and inside measurement of the wall were 60 mm and 1,760 mm, respectively (WF has no wall).

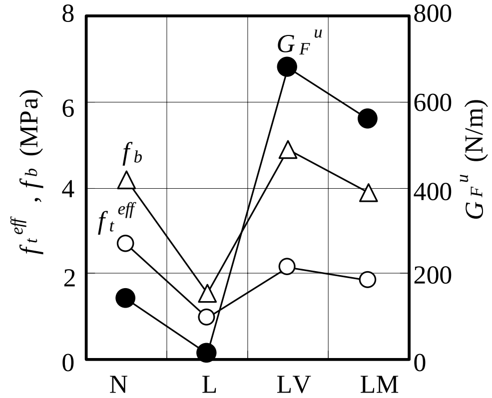

Figure 4: $G_F^u \cdot f_t^{eff} \cdot f_b$

Table 7: Material characteristics of reinforced bars

Type		Yield Strength (MPa)	Tensile Strength (MPa)	Young's Modulus (GPa)
Column Main Bars	D13	384	541	206
Column Hoops, Wall Bars	D6	335	631	201
Precast Bars	ϕ 3.2	—	662	—

Table 8: Specimens for horizontal loading tests

Specimen Type		WF	WN	WV	WL	WM
Column	Section	240×240mm				
	Main Bars	12-D13 Pg 2.65%				
	Hoop	D6 @50 Pw 0.53%				
Wall	Section	-	60×1760mm			60×392mm Precast 4pieces
	Bars		D6 @200 Ps 0.27%			φ3.2 @50 Ps 0.27%
	Concrete Mixture		N	LV	L	LM
Load	Vertical Force	1/6BDσ_B for each columns				
	Cycle R (times)	±1/6400(1),±1/3200(1),±1/1600(1), ±1/800(1),±1/400(1),±1/200(1), ±1/100(1),±1/50(1),+1/25(1)			±1/800(1),±1/400(1),±1/200(2), ±1/100(2),±1/50(2),+1/25(1)	

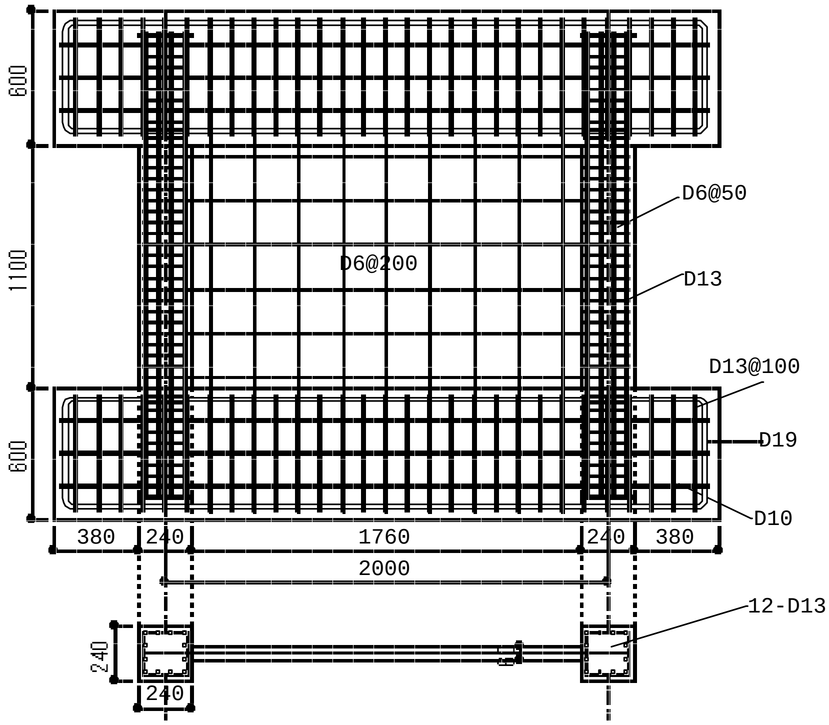

Figure 5: Details of specimens for horizontal loading test (WN, WV and WL)

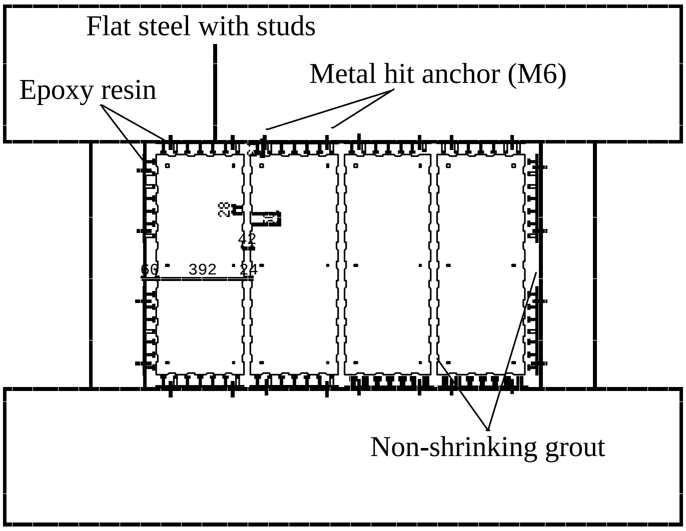

Figure 6: Method of installing column-beam frame with precast panels (WM)

12-D13 (SD 345) bars were used for the longitudinal bars in the columns. The additional bar ratio in the columns was 0.53%, assuming shear failure of the wall before shear failure of the columns.

Whereas normal concrete was placed monolithically in the WF and WN specimens, normal concrete was placed only in the column-beam frame of the WL and WV specimens, followed by placement of L and LV concretes, respectively, in the wall surrounded by the frame. Wall reinforcement was placed at the time of concreting for the column-beam frame. Indentations 20 mm in depth and 100 mm in width were provided in the frame to serve as cotters.

As for the WM specimen, precast panels of LM mortar were installed after constructing the column-beam frame (Figure 6). The installation procedure was as follows: Flat steel with studs was fixed to the frame with an epoxy adhesive. Precast panels having protruding cotters 9 mm in height, 50 mm in top width and 56 mm in bottom width at 84-mm spacing on its periphery were installed in position. Non-shrinking grout was filled in all joints.

Loading method:
Alternating and increasing loads were applied horizontally under a fixed vertical load. Figure 7 shows the loading equipment. A fixed vertical force, N (= 1/6BDσ_B, where BD: cross-sectional area of columns, σ_B:compressive strength of concrete) was applied to the tops of the column centers on both sides across the upper stub wall using two 100-tonf hydraulic jacks. The horizontal force was applied to the upper stub wall at its vertical center through loading jigs so that the loads from 200-tonf hydraulic jacks on both sides were equalized. The loads were applied by numbers of cycles given in Table 8, being controlled on a displacement basis. The story deformation angle, R, was determined by dividing the horizontal displacement δ by the height from the bottom of the wall to the vertical center of the upper stub wall (1,400mm).

Results:
Figure 8 shows the relationship between the shearing force and the story deformation angle obtained from the horizontal loading tests. The final state of failure is shown in Photo 1. The WF specimen reached the maximum yield strength when R was 1/67 rad., and retained a horizontal yield strength of over 200 kN when R was±1/25 rad. All the other specimens having a wall exhibited their maximum yield strengths at R values ranging from 1/250 to 1/200 rad.

Table 9 compares the results of the experiment. The horizontal yield strength ratios are based on the maximum yield strength of WN as 1.0. In this experiment, the horizontal yield strength ratio of WL, in which the compressive strength of the wall concrete matched that of WN, was as low as 0.86. Even that of WM, whose wall had a compressive strength 1.25 times higher than WN, was 0.93. All the specimens containing foamed aggregate concrete exhibited lower maximum yield strengths than WN, the normal concrete specimen. However, he maximum yield strength of these specimens was more than 2.6 times higher than that of WF having no wall, in both cases of integrated placing, such as WV and WL, and precast panels, such as WM. It is therefore

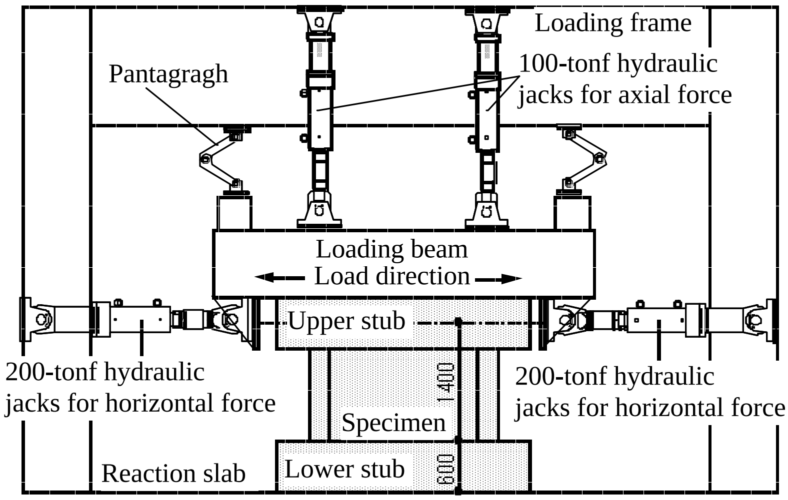

Figure 7: Loading apparatus for horizontal loading test

Table 9: Results of the experiment

Specimen Type	Direction	Maximum Yield Strength (kN)	Story Deformation Angle R (x10^{-3}rad.)	Horizontal Yield Strength Ratio	Failure Mode
WF	positive	245	14.74	0.27	Flexural Failure of Column
	negative	-244	-12.24		
WN	positive	922	5.06	1.00	Compressive Failure of Wall Concrete with Slip
	negative	-930	-3.97		
WV	positive	667	5.03	0.72	Shear Failure of Wall
	negative	-631	-5.02		
WL	positive	790	4.81	0.86	Shear Failure of Wall
	negative	-624	-4.08		
WM	positive	853	5.03	0.93	Shear Failure of Wall
	negative	-753	-5.02		

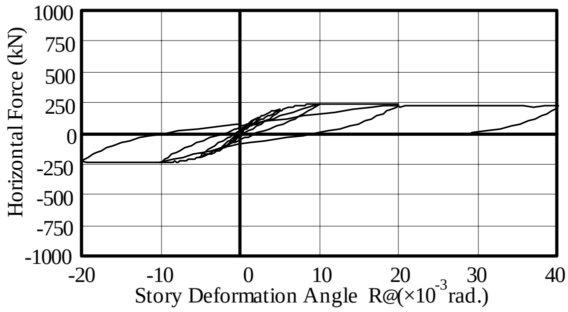

(1) WF

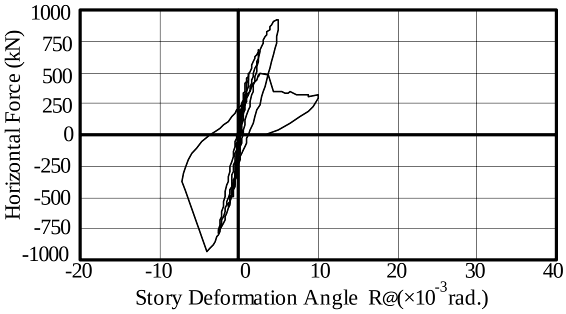

(2) WN

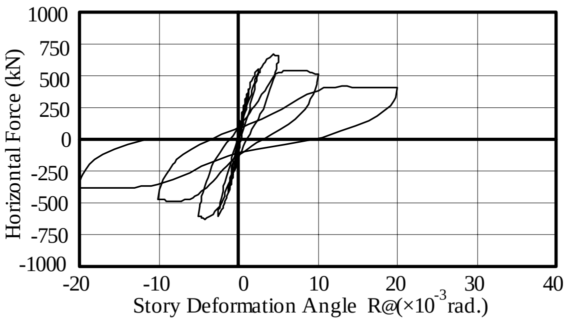

(3) WV

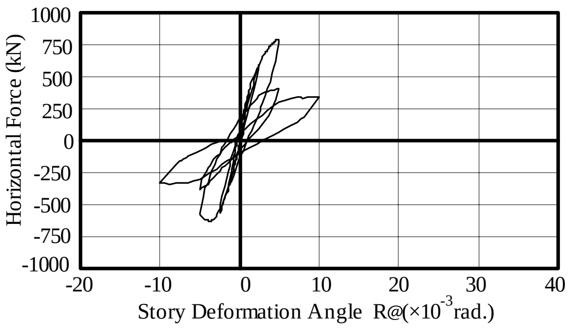

(4) WL

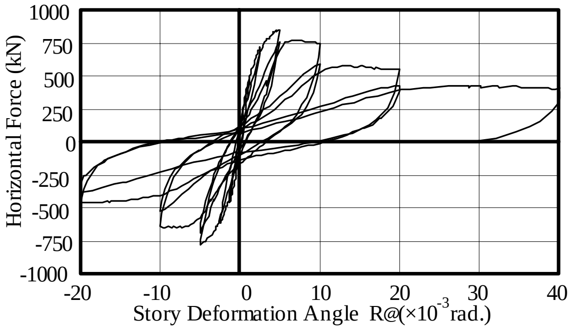

(5) WM

Figure 8: horizontal force - story deformation angle curve

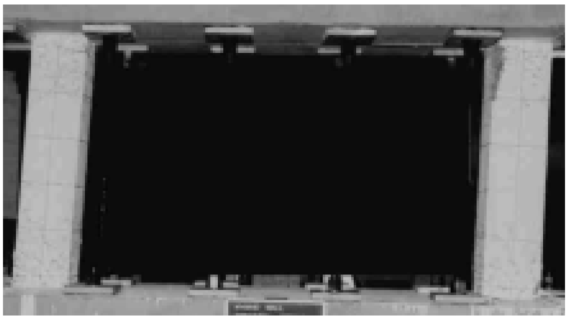

(1) WF

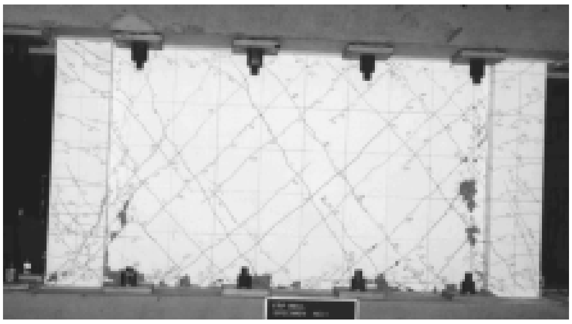

(2) WN

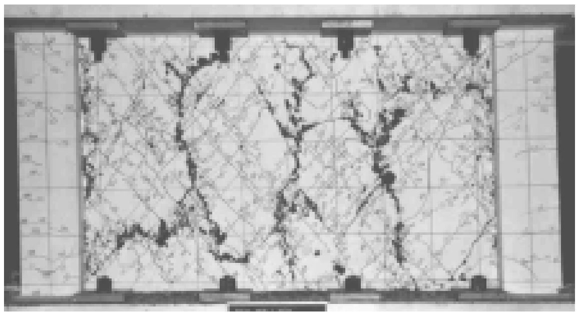

(3) WV

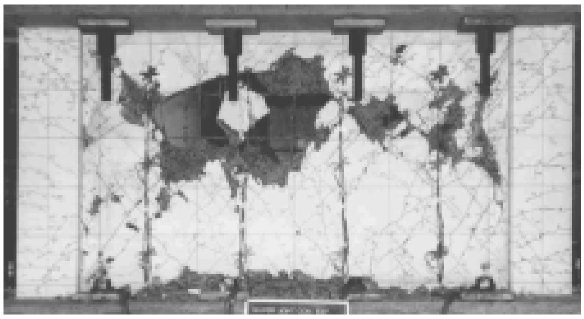

(4) WL

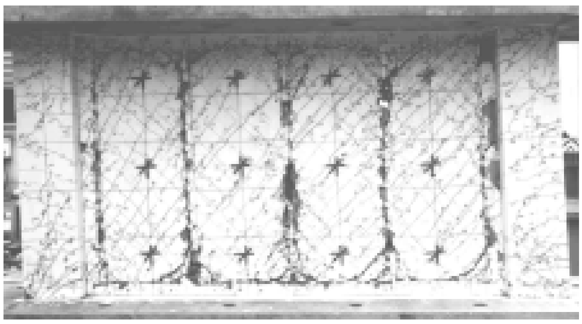

(5) WM

Photo 1: final state of failure

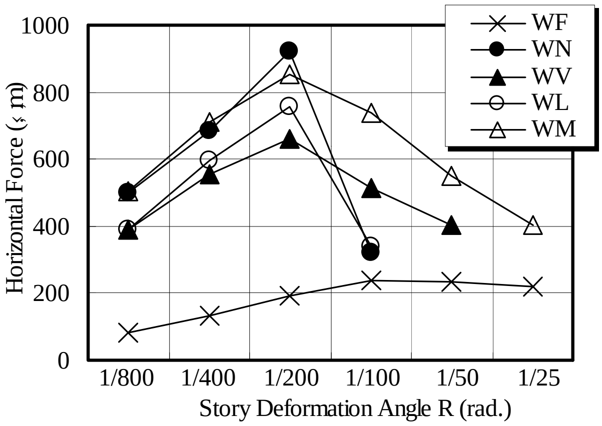

Figure 9: Horizontal Force at the time of maximum displacement for each cycle in positive.

concluded that concrete containing foamed waste glass aggregate is sufficiently functional as supplementary shear walls and that it can be used as precast panels.

Figure 9 shows the horizontal force at the time of maximum displacement for each cycle in the positive direction. The figure reveals that the yield strength of WN and WL abruptly decreased after R reached 1/200 rad near the maximum yield strength. However, the losses in the yield strength of WV and WM, which exhibited high ductility in the center-point loading test on notched beams, were relatively small. Accordingly, such high ductility materials, when applied to shear walls, are considered to prevent abrupt decreases in the horizontal yield strength under large shearing deformation.

CONCLUSIONS

Concrete containing foamed waste glass aggregate was subjected to center-point loading tests using notched beams and horizontal loading tests using wall specimens, which revealed the following:
(1) The ductility of foamed aggregate concrete is significantly improved by the inclusion of vinylon fibers.
(2) Shear walls made of foamed aggregate concrete have a yield strength more than 2.6 times higher than column-beam frames without walls. Wall panels of such concrete are sufficiently functional as supplementary shear walls and also feasible in the form of precast panels.
(3) Inclusion of vinylon fibers improves the ductility of foamed aggregate concrete shear walls, enabling them to avoid abrupt post-peak losses in the yield strength.

The authors would like to thank Crystal Clay Co., Kuraray Co. and Pozzolith Bussan Co. for supplying the test materials.

REFERENCES

RILEM Draft Recommendation (1985), "Determination of the Fracture Energy of Mortar and Concrete by Means of Three-point Bend Test on Notched Beams", *Materials and Structures*, Vol.18, No.106, pp.285-290
Kitsutaka, Y., Kamimura, K. and Nakamura, S. (1993), " Poly-linear approximation analysis of tension softening diagram for concrete", *Journal of Structural and Construction Engineering, Architectural Institute of Japan*, No.453 pp.15-25. (in Japanese)
Kitsutaka, Y. (1997), " Fracture parameters by polylinear tension-softening analysis", *Journal of Engineering Mechanics, ASCE*, 123(5), pp.444-450
Kitsutaka, Y. and Oh-oka, T., (1998), "Fracture parameters of high-strength fiber reinforced concrete based on poly-linear tension softening analysis", *Fracture Mechanics of Concrete Structures*, (FRAMCOS-3, edited by Mihashi, H. and Rokugo, K.), pp.455-464